Analysis of Orbital Hybridization in the Magnetoelectric $YMnO_3$ Crystal From First Principles Calculations

Adilmo Francisco Lima and Milan V. Lalic

Departamento de Física, Universidade Federal de Sergipe, 49100-000 São Cristóvão-SE, Brazil

We performed first-principles band-structure calculations on multiferroic hexagonal $YMnO_3$ to study the characteristics of Mn-O and Y-O chemical bonds in the vicinity of ferroelectric (FE)—paraelectric (PE) phase transition. Both the FE and the PE crystal structures were successfully reproduced and considered paramagnetic ones. Exchange-correlation effects between electrons were treated by the recently developed modified Becke-Johnson (mBJ) approach which enabled successful reproduction of experimental band gap in the FE phase and predicted a small band gap in the PE phase. Analysis of the resulting electronic structures in both phases indicates that Mn-O bonds do not suffer significant changes during the PE-FE phase transition, while the Y-O bonds become more covalent, with clear signs of hybridization between Y $4d_z^2$ and the O p_z orbitals.

Index Terms—**Density functional theory (DFT), electronic properties, manganites, multiferroics.**

I. Introduction

THE hexagonal $YMnO_3$ (h-YMO) is one of the most studied magnetoelectric materials because of its suitability for usage in ferroelectric memories and due to the intriguing coexistence of ferroelectricity and magnetism [1]–[3]. It has a high ferroelectric-paraelectric transition temperature ($T_c \sim 1258$ K), and a low antiferromagnetic-paramagnetic transition temperature ($T_n \sim 75$ K). For $T < T_n$ the h-YMO is simultaneously antiferromagnetic (with noncollinear Mn spins ordered in a triangular arrangement [4]) and ferroelectric, exhibiting a clear multiferroic characteristic. At temperatures between T_n and T_c, the h-YMO is in the ferroelectric (FE) phase, having the noncentrosymmetric structure described by the space group $P6_3cm$ and electric polarization along the c-axis. In its paraelectric (PE) phase, above T_c, the h-YMO has a centrosymmetric structure described by the space group $P6_3/mmc$ [5].

Aiming to understand the origin of magnetoelectric properties of this compound, significant experimental and theoretical efforts have been made so far [6]–[8]. As a result of these works, it was established that the mechanism that causes ferroelectricity in the h-YMO is different from the mechanisms in other multiferroic materials such as $BiFeO_3$ (where the chemical behavior of the Bi $6s^2$ lone pair plays an important role [9]) and $TbMnO_3$ (where the principal mechanism is spin frustration magnetic ordering [10]). What is the exact nature of the driving force of ferroelectricity in the h-YMO, however, is still a matter of debate in the literature [11]–[14].

Filippetti and Hill [11] proposed the Mn d^0-ness model, based on results of their first principles density functional theory (DFT) calculations. They stated that the h-YMO ferroelectric distortion is due to unoccupied Mn $3d_z^2$ orbital that hybridize with the O 2p states. Van Aken *et al.* [12] used a combination of single-crystal X-ray diffraction and DFT calculations have suggested that the ferroelectricity is generated by the geometric effect rather than by hybridization. Cho *et al.* [13], however, performed polarization dependent X-ray absorption spectroscopy and showed that the Y 4d states are strongly hybridized with the O 2p states. By an analogy with ferroelectric electronic origin of the $BaTiO_3$ crystal [15], they suggested the Y d^0-ness model for h-YMO compound, although they have not described in detail how it is realized. Two years later, Kim *et al.* [16] investigated experimentally the Y-O hybridization of the h-YMO crystal in the temperature range around T_c and gave evidence of an increase of orbital hybridization between the Y and O ions along the polar c-axis. More recently, Liu *et al.* [14] proposed another mechanism for the ferroelectric origin of the h-YMO that might be associated with the charge transfer from the Y-O bonds to the Mn-O bonds.

The main goal of the present work is to investigate how the chemical bonds between the Mn 3d and O 2p, and the Y 4d and O 2p orbitals change when the h-YMO suffers a phase transition from the PE to the FE structure. Towards this aim, we performed first principles DFT calculations of the h-YMO crystal in both paraelectric and ferroelectric phases, both being treated in the paramagnetic state. In our calculations we employed for the first time one of the most advanced approaches to treat exchange-correlation effects between electrons in insulators and semiconductors, the Tran-Blaha modified Becke-Johnson (TB-mBJ) approach [17], as well as its respective improvement [18]. By careful analysis of calculated electronic structure we showed that the Y $4d^1$- and the O $2p^2$-states suffer a rehybridization during the PE $\rightarrow$ FE phase transition, thus supporting the Y d^0-ness model proposed in [13].

II. Calculation Details and Structural Optimization

All calculations were carried out using a full potential linear augmented plane wave (FP-LAPW) method [19] as embodied in WIEN2k computer code [20]. In this method, the electronic wave functions, charge density and crystal potential are expanded in spherical harmonics inside the nonoverlapping spheres centered at each nuclear position (atomic spheres with

Manuscript received February 14, 2013; revised March 20, 2013; accepted March 26, 2013. Date of current version July 23, 2013. Corresponding author: A. F. Lima (e-mail: adilmol@ufs.br).

Color versions of one or more of the figures in this paper are available online at http://ieeexplore.ieee.org.

Digital Object Identifier 10.1109/TMAG.2013.2256112

TABLE I
CALCULATED EQUILIBRIUM LATTICE CONSTANTS AND SELECTED INTERATOMIC DISTANCES (IN Å) IN H-YMO CRYSTAL COMPARED TO EXPERIMENTAL DATA. PARENTHESIS SHOW NUMBER OF CORRESPONDING EQUIVALENT BONDS

	This work	Exper.[5]		This work	Exper.[4]
Ferroelectric			Paraelectric		
a	5.995	6.155	*a*	3.499	3.618
c	11.646	11.403	*c*	11.402	11.340
Mn – O1 (x1)	1.885	1.850	Mn – O1 (x3)	2.020	2.089
Mn – O2 (x1)	1.876	1.878	Mn – O2 (x2)	1.870	1.865
Mn – O3 (x1)	2.047	1.996			
Mn – O4 (x2)	1.986	2.097			
Y1 – O3 (x1)	2.328	2.345	Y – O1 (x2)	2.851	2.835
Y2 – O4 (x1)	2.497	2.459			

radii RMT) and in plane waves in the rest of the space (interstitial region). The choice for the atomic sphere radii (in atomic units) was 2.0 for Y, 1.8 for Mn and 1.5 for O. Inside atomic spheres the partial waves were expanded up to $l_{\max} = 10$, while the number of plane waves in the interstitial was limited by the cutoff at $\mathrm{K}_{\max} = 7.0/\mathrm{RMT}$. The charge density was Fourier expanded up to $\mathrm{G}_{\max} = 14$. A mesh of 5 k-points in the irreducible part of the Brillouin zone was used. Tests with more k-points were made, not leading to essentially different results. The Y 4s, 4p, 4d, 5s the Mn 3s, 3p, 3d, 4s and the O 2s, 2p electronic states were considered valence ones. Exchange and correlation effects in our calculations were treated in a two-fold manner. First, we performed a relaxation of hexagonal lattice parameters and all atomic positions for both FE and PE phases of the h-YMO using the generalized gradient approximation with Perdew-Burke-Ernzenhof parameterization (GGA-PBE) [21]. Within the relaxed structures all the atoms experience forces less than 2 mRy/a.u. Then, we calculated electronic bands for these optimized structures employing the semi-local exchange potential appropriate for strongly correlated electronic systems: Tran-Blaha modified Becke-Johnson (TB-mBJ) potential [17] for the FE phase, and the improved variance of the TB-mBJ potential [18] for the PE phase. The improved TB-mBJ potential has been applied in order to open a gap in the PE phase and correct the original TB-mBJ which resulted in metallic solution for it. The self-consistent calculations for both phases of $YMnO_3$ were performed on the same level of precision and good convergence of the results has been achieved (less than 10^{-4} Ry and $10^{-5}e$ for energy and charge convergence, respectively).

Fig. 1(a) and (b) presents both hexagonal FE ($P6_3cm$) and PE ($P6_3mmc$) fully optimized crystal structures of the h-YMO. The primitive unit cells of the PE and the FE phase contain 10 and 30 atoms, respectively. Table I summarizes the calculated lattice constants and some selected interatomic distances in the Mn and Y first coordination spheres and compares them with the corresponding experimental values. As it can be seen, the overall agreement between theoretical and experimental data is good. This means that the characteristics of both distinct crystal

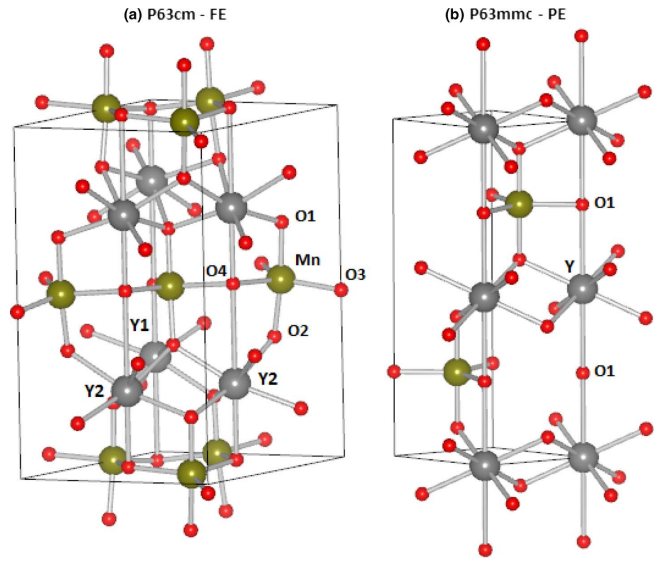

Fig. 1. Fully optimized crystal structures of h-YMO in its (a) ferroelectric and (b) paraelectric phase. In the FE phase there are two nonequivalent Y^{3+} ions (Y1 and Y2), while in the PE structure all Y^{3+} ions are crystallographically equivalent. In both FE and PE crystal structures the Y^{3+} ions are surrounded by 8 O^2 ions.

phases have been preserved in our calculations. Special attention should be paid to the fact that the FE structure can be generated from the higher symmetry PE structure by the loss of the mirror symmetry perpendicular to the c-axis, resulting in tilted MnO_5 bipyramids and unequal Y(1,2)—O(3,4) bond lengths. This fact is clearly reproduced by our first-principles calculations, serving as an additional evidence of adequacy of the presented theoretical approach.

III. ELECTRONIC STRUCTURE

Fig. 2 shows the calculated total electronic density of states (TDOS) for the h-YMO compound in its PE and FE phases. For both phases our calculations lead to semiconductor solutions. The calculated band gap in the FE phase is 1.6 eV, which is coincident with the estimated experimental optical gap [22]. The

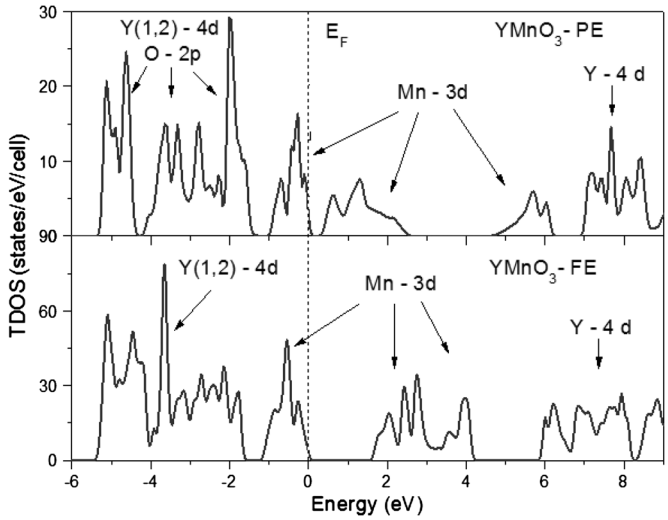

Fig. 2. TDOS of h-YMO in the PE and FE phase. Predominant orbital character of some bands is denoted. Vertical dot line indicates the Fermi level.

calculated gap for the PE structure is found to be 0.4 eV. Although we did not find any published experimental facts about electronic structure of the h-YMO in the PE phase, we supposed that it should present a nonzero band gap having in mind that the compound is an oxide and possesses a large gap in the FE phase. It should be stressed that the GGA-PBE approach leads to metallic solutions for both the FE and the PE phases, which is certainly wrong at least for the FE structure. The error occurs due to well-known deficiency of the GGA (or LDA) treatment of the exchange and correlation effects between electrons [17]. This fact imposed the necessity to treat these effects in a more realistic way, which has been performed in the present work. The TB-mBJ approach [17] reproduced the correct gap for the h-YMO FE phase, while the improved TB-mBJ potential [18] opened a small gap in the case of the h-YMO PE phase. Both structures (phases) were considered nonmagnetic ones, which is a reasonable supposition at such high temperatures that separate the FE from the PE phase.

Fig. 2 demonstrates that the $YMnO_3$ TDOS differs significantly in the two different phases, mostly because of substantial rearrangement of the Y and the Mn d-states. Going from the PE to the FE phase, two principal changes could be noted. The first one is that the empty Mn d-states, separated in two bands in the PE structure, concentrate themselves in unique energy range from 1.6 to 4.1 eV in the FE structure. The second one is a change of the TDOS within the valence band, in which the PE phase contains the most prominent peak centered at -2 eV while in the FE phase the most prominent peak is centered at -3.8 eV. Both of these changes can be explained by analysis of partial electronic density of states (PDOS), which is presented in Fig. 3.

Changes within the conduction band can be understood in terms of the crystal field splitting. In both, the FE and PE structures the local symmetry of the Mn is bipyramidal, thus the energy of its 3d orbital is split into two doublets $e_{1g}(xz, yz)$ and $e_{2g}(x^2 - y^2, xy)$, and one singlet $a_{1g}(z^2)$. This splitting is clearly seen from the Mn 3d PDOS in the PE phase (Fig. 3), where the a_{1g} orbital has the highest energy due to the fact that

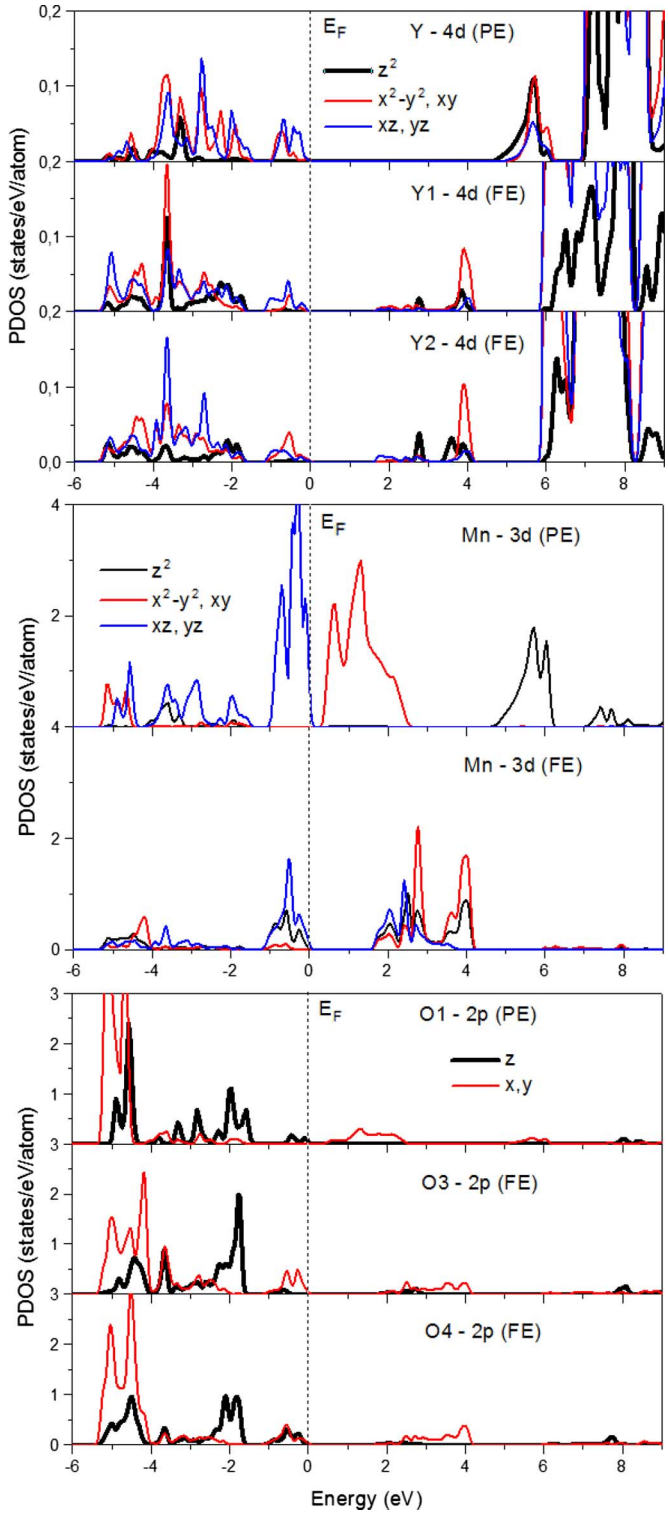

Fig. 3. The PDOS of the h-YMO in the PE and FE phase. Vertical dot line indicates the Fermi level.

the apical oxygens O_T (situated along the $c-$, i.e., z-axis) are closer to the Mn ion than the in-plane O_P ones. In the FE phase the $Mn-O_T$ and the $Mn-O_P$ distances are not so different (see Fig. 1 and Table I), thus the energy splitting between the Mn d-orbitals become smaller, resulting in formation of a unique band. The chemical bonds between the Mn and neighboring O ions are, however, altered very little because within the energy

range where the Mn 3d-states are abundant there are very few O states at disposal for hybridization.

On the other hand, changes of the DOS within the valence band can be related to changes of the chemical bonds between the Y ions and their neighboring apical oxygens. Within the PE structure the occupied Y 4d-states (0.279 electrons within the Y atomic sphere) are spread over the whole valence band, without any peak that is distinguished from the others. They consist of all types of d-states except the d_z^2 ones that are almost empty (0.026 electrons). Within the FE structure, however, it is formed a narrow and sharp peak with a clear Y 4d and O 2p character, centered at approximately -3.8 eV. It contains significant amount of the Y d_z^2 states whose increasing presence can be perceived over a whole valence band (within the Y1 atomic sphere there are 0.296 d-electrons, being 0.059 in the d_z^2 states). Appearance of this peak indicates hybridization between the Y d_z^2 and the O $2\mathrm{p}_z$ orbitals which changes the character of the bond between the Y's and their apical oxygens. Namely, filling of the Y d_z^2 orbital occurs because the charge distributed along the Y-O bond in the z-direction moves towards the Y ion, thus increasing the covalent character of this bond when compared to the same bond in the PE phase. Therefore, our calculations indicate that the PE $\rightarrow$ FE transition is accompanied by re-hybridization between the Y and O orbitals. This effect is very similar to the one that occurs with the Ti-O bonds in $BaTiO_3$ and explains its ferroelectricity [15]. By analogy, we conclude that hybridization between the Y 4d and O 2p states might be responsible for ferroelectricity in the $\mathrm{h}-YMnO_3$, supporting this way the Y d^0-ness model as it was proposed in [13].

IV. Conclusion

In this paper, we present the first principle study of the hexagonal $YMnO_3$ (h-YMO) multiferroic compound in its PE and ferroelectric FE phases using the DFT-based FP-LAPW method and treating exchange and correlation effects by the recently developed TB-mBJ approach. Both structures were simulated in the paramagnetic state. The main objective was to investigate how the FE $\rightarrow$ PE phase transition influences orbital hybridizations between the Mn and O and Y and O orbitals. A careful analysis of the h-YMO DOS in both phases shows that the Mn-O bond character does not suffer significant changes while the Y-O bonds become more covalent due to hybridization between the Y $4\mathrm{d}_z^2$ and the O $2\mathrm{p}_z$ orbitals. This fact indicates that Y-O hybridization could be responsible for ferroelectricity of the h-YMO compound, supporting the d^0-ness model which has been successfully applied in the case of the $BaTiO_3$ compound.

Acknowledgment

This work was supported in part by the CNPq, CAPES and FAPITEC (Brazilian funding agencies).

References

[1] E. F. Bertaut and M. Mercier, *Phys. Lett.*, vol. 5, pp. 27–29, 1963.
[2] M. Fiebig, T. Lottermoser, D. Frohlich, A. V. Goltsev, and R. V. Pisarev, *Nature*, vol. 419, pp. 818–820, 2002.
[3] W. Eerenstein, N. D. Mathur, and J. F. Scott, *Nat. Rev.*, vol. 442, pp. 759–765, 2006.
[4] A. Munoz, J. A. Alonso, M. J. Martínez-Lope, M. T. Casaís, J. L. Martínez, and M. T. F. Díaz, *Phys. Rev. B*, vol. 62, pp. 9498–9510, 2000.
[5] A. S. Gibbs, K. S. Knight, and P. Lightfoot, *Phys. Rev. B*, vol. 83, p. 094111, 2011.
[6] S.-W. Cheong and M. Mostovoy, *Nat. Mat.*, vol. 6, pp. 13–20, 2007.
[7] C.-W. Nan, M. I. Bichurin, S. Dongb, D. Viehland, and G. Srinivasan, *J. Appl. Phys.*, vol. 103, p. 031101, 2008.
[8] T.-H. Arima, *J. Phy. Soc. Japan*, vol. 80, p. 052001, 2011.
[9] P. Ravindran, R. Vidya, A. Kjekshus, H. Fjellvag, and O. Eriksson, *Phys. Rev. B*, vol. 74, p. 224412, 2006.
[10] T. Kimura, T. Goto, H. Shintani, K. Ishizaka, T. Arima, and Y. Tokura, *Nature*, vol. 426, pp. 55–58, 2003.
[11] A. Filippetti and N. A. Hill, *Phys. Rev. B*, vol. 65, p. 195120, 2002.
[12] B. B. van Aken, T. T. M. Palstra, A. Filippetti, and N. A. Spaldin, *Nat. Mat.*, vol. 3, pp. 164–170, 2004.
[13] D.-Y. Cho *et al., Phys. Rev. Lett.*, vol. 98, p. 217601, 2007.
[14] S.-H. Liu *et al., AIP Advances*, vol. 1, p. 032173, 2011.
[15] R. E. Cohen, *Nature*, vol. 358, pp. 136–138, 1992.
[16] J. Kim, K. C. Cho, Y. M. Koo, K. P. Hong, and N. Shin, *Appl. Phys. Lett.*, vol. 95, p. 132901, 2009.
[17] F. Tran and P. Blaha, *Phys. Rev. Lett.*, vol. 102, p. 226401, 2009.
[18] D. Koller, F. Tran, and P. Blaha, *Phys. Rev. B*, vol. 85, p. 155109, 2012.
[19] O. K. Andersen, *Phys. Rev. B*, vol. 12, pp. 3060–3083, 1975.
[20] P. Blaha, K. Schwarz, G. K. H. Madsen, D. Kvasnicka, and J. Luitz, An *Augmented Plane Waves+Local Orbital Program for Calculating Crystal Properties,* Karlheinz Schwarz, Techn. Universitat Wien, Austria, 2001.
[21] J. P. Perdew, K. Burke, and M. Ernzerhof, *Phys. Rev. Lett.*, vol. 77, pp. 3865–3868, 1996.
[22] A. M. Kalashinikova and R. V. Pisarev, *JETP Lett.*, vol. 78, pp. 143–147, 2003.